

Ionization of Excited Hydrogen Atoms by Microwave Fields: A Test Case for Quantum Chaos

R. Blümel

Max-Planck-Institute for Quantum Optics D-8046 Garching, FRG

and

U. Smilansky

Department of Nuclear Physics, The Weizmann Institute, Rehovot 76100, Israel

Abstract

Analytical formulas for the critical ionization field of the microwave driven H-atom are derived. Good agreement with measured ionization fields is obtained.

1. Introduction

Much of our understanding of the quantum dynamics of classically chaotic systems is derived from the study of the quantized standard map [1, 2] (referred to also as the “kicked rotor”). The classical treatment of this problem [3] displays the most important features of chaos in classical Hamiltonian systems. The quantum mechanics of the kicked rotor was discussed by Dr Fishman in the previous talk, with special emphasis on the relation between classical diffusion and quantal localization. Is this result general and characteristic of all the quantum dynamics of classically chaotic systems? To investigate this important problem, much effort was recently directed to study the quantal description of other classically chaotic systems. Among these, the excitation [4, 5] and further ionization [5–11] of highly excited hydrogen atoms by microwave fields plays a very prominent role. In the present contribution we shall discuss the quantal and classical dynamics of this system, with the aim of shedding some more light on the questions raised above. The special standing of this particular problem can be attributed to the following elements: Classically, for any given initial state of the atom, there is a critical field strength above which the classical trajectories become chaotic and energy is transferred from the field to the atom by a characteristic diffusion mechanism [12–14]. The ionization occurs subsequently, and its onset and rate probes directly the way by which the atom is excited. A closer look at this system shows that in many important features it differs from the kicked rotor. Thus, the comparison of the quantal treatment of both cases can test in a meaningful way whether there are any universal features in the quantal behavior which are common to systems whose classical dynamics is chaotic.

The study of the hydrogen atom in a microwave field is important and interesting in its own right. Extensive measurements of the ionization signals are available [5–11] which occasionally display features which were explained only recently [15–17]. Our understanding of the response of the simplest atom to strong external fields is also a prerequisite

for the study of the behavior of more complicated atoms in similarly extreme environments [18].

We shall focus the present discussion on properties and observables which are directly related to the experimental data obtained recently by P. Koch and his group in Stony Brook [8–11]. In these experiments, a beam of neutral atoms is prepared in a highly excited state with principal quantum numbers in the range $32 \leq n \leq 90$. The beam passes through a microwave cavity operated at a frequency of 9.92 GHz, and the passage time corresponds to approximately 300 cycles of the field. The entrance and exit holes in the cavity cause fringe fields and hence the field experienced by the atom is switched gradually over a period of approximately 80 cycles. After leaving the cavity, the fraction of ionized atoms is monitored and gives the ionization probability $P(\varepsilon; n)$ which depends on the applied field strength ε and the initial state n . The dependence of the ionization probability on ε for a constant n will be referred to as an ionization curve, and a few examples are shown in Fig. 1. The onset of ionization is rather abrupt and can be characterized experimentally by the field ε_c at which the ionization probability reaches 10%. The dependence of ε_c on n and the details of the ionization curve are the experimental observables which will be addressed in the following classical and quantum theories. It was observed that the salient features of the ionization process can be very well described within a model where the electron is confined to move in one dimension parallel to the applied electric field [19, 20]. This model can be rigorously justified when the initial state is an extremal Stark level [20]. It is less obvious why the 1-dim. model is so successful when the initial state is unpolarized, although some plausible arguments can be put forward in support of this observation. We shall use the 1-dim. model throughout this paper.

The 1-dim. Hamiltonian is written as:

$$H(z, t) = H_0 + \varepsilon z \sin(\omega t)$$

$$H_0 = \begin{cases} \frac{p^2}{2} - \frac{1}{z} & z > 0 \\ \infty & z \leq 0 \end{cases} \quad (1.1)$$

It is supplemented by the boundary condition of elastic reflection at $z = 0$. In equation (1.1) as well as in the rest of the paper, atomic units are used for the field strength ε and the frequency ω . An important feature of the Stony Brook data

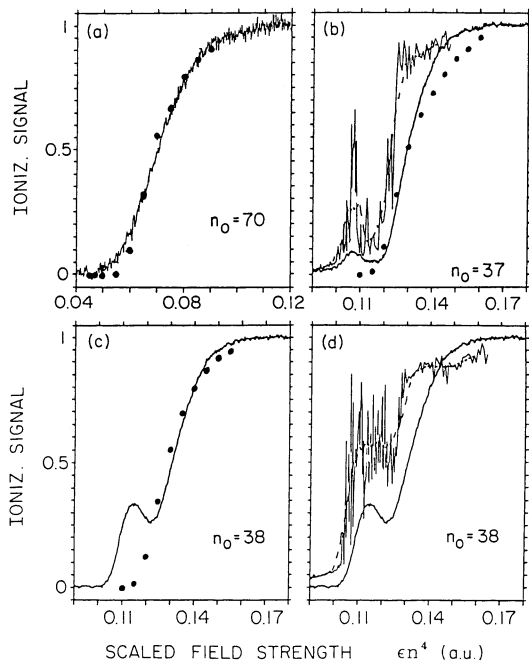


Fig. 1. Experimental and theoretical ionization curves. (a) $n_0 = 70$, (b) $n_0 = 37$, (c) and (d) $n_0 = 38$. Heavy line: experiment [8–11]. Full dots: classical 3-dim. theory [23, 24]. Thin line: quantum mechanical calculations [16]. Dashed line: quantum mechanical results convoluted with the experimental field profile.

is that the ratio between the field frequency ω and the classical Kepler frequency $1/n^3$ obeyed $\omega n^3 \approx 1$ for all initial conditions. The theoretical discussion will be confined to this range of parameters. A recent paper by Casati *et al.* [21] addresses the complementary regime with $\omega n^3 > 1$.

2. Classical theory

Detailed numerical solutions of the classical equations of motion were recently carried out and compared with the experimental data [9, 22–26]. The classical theory accounts surprisingly well for most of the features of the ionization curves [22–24] (see Fig. 1) and the dependence of the threshold fields on the initial state n [23–26] (see Fig. 2). The classically calculated $\varepsilon_c(n)$ reproduce structures observed when the field and the Kepler frequencies are rationally

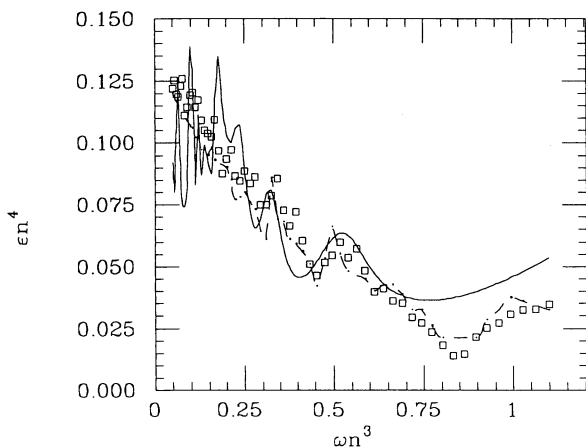


Fig. 2. Experimental and theoretical dependence of the (scaled) critical ionization field εn^4 on the (scaled) frequency ωn^3 . Squares: experiment [8–11]. Dashed line: classical numerical calculations [25, 26]. Full line: classical perturbation theory. (“Quantum version” of equation (2.7)).

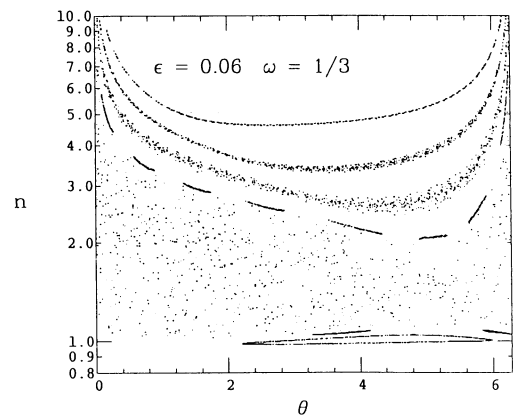


Fig. 3. Stroboscopic phase-space portrait, showing, as n increases, the transition from regular motion to chaos to z -dominated motion.

related, i.e., when $\omega n^3 = 1, 1/2, 1/3, 2/5$ etc. The classical theory is unable to explain non-monotonic structures which appear in the ionization curves for some initial n values (see e.g., Fig. 1(c)). We shall show that these are due to genuine quantum effects.

The discussion of chaos in conservative classical systems makes sense only as long as configuration space is bounded. In this sense the hydrogen atom differs from the kicked rotor: the electron may also be unbounded. Chaos is observed, however, within the bounded (negative energy) section of phase-space and we shall confine our attention to it. There, the natural representation of the classical dynamics is in terms of action-angle variables. The Hamiltonian reads now:

$$H = -\frac{1}{2n^2} + \varepsilon \cdot z(n, \Theta) \cdot \sin(\omega t)$$

$$z(n, \Theta) = \frac{3}{2}n^2 \left(1 - \frac{4}{3} \sum_{k=1}^{\infty} x_k \cos(k\Theta) \right) \quad (2.1)$$

where $x_k = J'_k(k)/k \approx 0.41/k^{5/3}$.

It should be pointed out that the Hamiltonian (2.1) is equivalent to the Hamiltonian (1.1) *only* within the *bounded* part of phase-space, that is, when $p^2/2 - 1/z < 0$. The canonical transformation $(p, z) \leftrightarrow (n, \Theta)$ is singular on the line $p^2/2 - 1/z = 0$, where $n = \infty$ and the conjugate angle Θ cannot be defined. Therefore the Hamiltonian (2.1) does not uniquely describe the dynamics in the truncated phase-space and has to be supplemented by a boundary condition. Once a trajectory reaches $n = \infty$, the passage through this singular point is easily deduced from the requirement that z is continuous while p changes its sign. This boundary condition is the most natural choice and guarantees that there is no flow out of the bounded part of phase-space.

Figure 3 is a stroboscopic phase-space portrait of some typical classical trajectories obtained by solving the classical equations of motion in the bound space and marking by a dot the position of a trajectory at integer multiples of the driving field period. In the low n domains one sees regular, quasi-periodic orbits. At higher n values the typical structures of periodic orbits, confining KAM trajectories and island chains are replaced by regions of apparent disordered motion (Fig. 4 shows some of these structures in further detail). When n is increased even further, one observes that the chaotic trajectories are replaced by U-shaped structures. They start as rather diffused belts but as n increases further, the trajectories become more regular.

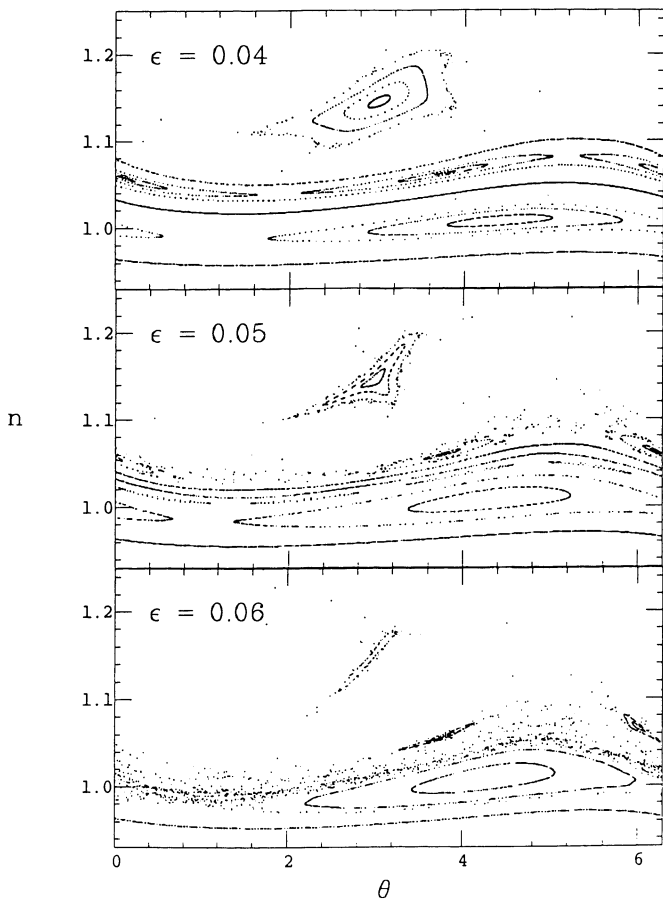


Fig. 4. Phase-space portraits of the $k/m = 1/3$ -resonance as a function of ε for driving frequency $\omega = 1/3$. (a) $\varepsilon = 0.04$, (b) $\varepsilon = 0.05$, (c) $\varepsilon = 0.06$.

A simple explanation for this phenomenon is offered by observing that in the Hamiltonian (2.1) the function $z(n, \Theta)$ increases quadratically with n while the unperturbed Hamiltonian decreases as $1/n^2$. Hence, at large n , the trajectories follow closer and closer the lines of constant $z(n, \Theta)$. The existence of this approximate constant of the motion is the cause of the regularization of the higher energy dynamics. In contrast with the rotor case, we see that chaos is confined to a rather narrow domain in phase-space. A quantitative discussion of the transition from the chaotic to the constant $z(n, \Theta)$ dominated dynamics can be carried out, but will not be pursued in the present lecture. We shall come back to this question when we analyze the quantum description.

In order to discuss the ionization, we must consider the dynamics in the entire phase-space and allow the electron to drift also to the positive energy domain. We find that the basic structures displayed in Fig. 3 characterize the dynamics even when the electron motion is unrestricted. An ionizing trajectory, however, dwells only during a finite amount of time in any of these structures before it escapes to the continuum. It turns out that the barrier against ionization are the KAM trajectories which separate the regular unperturbed motion at low n values from the chaotic domain. Once there, ionization eventually occurs. Thus, if the atom is initially in a given n state, we should calculate the field value at which the KAM trajectory just above n is breaking. This field should be compared with the ionization threshold field measured experimentally.

This scenario is illustrated in Fig. 4. The phase-space

portraits displayed in this figure show how the KAM trajectory between the $1/3$ and $2/5$ resonances breaks when the field strength is increased. Note how rapidly the regular phase-space in the vicinity of the $1/2$ resonance is diminishing.

We shall derive now simple analytical estimates for the threshold field mentioned above. We shall concentrate on the domain $\omega n^3 < 1$, since most of the experimental data fulfills this condition. This implies that the electron revolves around the atom much faster than the period of the driving field. To lowest order the Θ -dependent terms in the Hamiltonian (2.1) will average out during a field cycle. The Θ -independent term, however, will have an appreciable effect on the dynamics. Adding this term to the free atom Hamiltonian and solving the resulting equations of motion we see that n is unchanged while

$$\Theta = \Theta_0 + \frac{t}{n^3} - \frac{3\varepsilon n}{\omega} \cos(\omega t) \quad (2.2)$$

This suggests to introduce new action-angle variables $I = n - \bar{n}$ and $\xi = \Theta - t/\bar{n}^3 + 3\bar{n} \cos(\omega t)/\omega$ in the vicinity of a resonance $\omega \bar{n}^3 = k/m$. Keeping only the lowest non-vanishing orders in I and ξ , the Hamiltonian (2.1) can be transformed to a time-independent pendulum Hamiltonian [3]. Estimating the trapping region of the pendulum, we obtained an analytical result for the half-width of $\omega n^3 = 1/m$ -type resonances [27]:

$$\Delta n = 0.35 \frac{n}{(m\gamma)^{1/4}} \left\{ \frac{1-\gamma}{3\varepsilon n^4} e^\gamma \right\}^{m/2}; \quad \gamma = \sqrt{1-9(\varepsilon n^4)^2} \quad (2.3)$$

It is easily checked that the half-width of the primary resonances in Fig. 4 is indeed given by (2.3) to a very good accuracy. Strong ionization will occur if the half-width of the primary resonances reaches the location of the $2/(2m-1)$ -type resonances (see Fig. 4), which are a distance

$$\Delta n = \frac{1}{\omega^{1/3}} \left[\frac{1}{(m-1/2)^{1/3}} - \frac{1}{m^{1/3}} \right] = \frac{1}{6} n(\omega n^3) \quad (2.4)$$

away. Equating (2.3) and (2.4), we can solve for the critical ionization fields, which for $\omega n^3 = 1/m$, $m = 2, \dots, 10$ reproduce the measured ionization fields to better than 30%. For still smaller frequencies the deviations become larger. They reach $\approx 60\%$ at $\omega = 1/20$ (which corresponds to $n_0 = 32$ in the experiments), and for $\omega \rightarrow 0$ the calculated ionization fields are a factor 2 higher than the known static ionization fields.

The approach just outlined is applicable only at quite a coarse, discrete set of (resonant) frequencies. In order to interpolate between the resonance frequencies, we use a different approach. Inserting (2.2) into the exact equation for \dot{n} and integrating over a complete cycle of the microwave field, we obtain the spread in n as a function of the angle Θ_0 :

$$\begin{aligned} \Delta n(\Theta_0) &= \int_0^{2\pi/\omega} \dot{n} dt \\ &= \frac{8}{3} \omega^2 n \sum_{k=1}^{\infty} x_k \sum_{s=1}^{\infty} \frac{s^2}{(k/n^3)^2 - (s\omega)^2} J_s \left(\frac{3\varepsilon n k}{\omega} \right) \\ &\quad \times \sin \left(k\Theta_0 - s \frac{\pi}{2} + \frac{\pi k}{\omega n^3} \right) \sin \left(\frac{\pi k}{\omega n^3} \right) \end{aligned} \quad (2.5)$$

If we denote by “ $\langle \rangle$ ” the average over the angles Θ_0 , we get for the mean square spread in n :

$$\langle (\Delta n)^2 \rangle = \frac{32}{9} n^2 (\omega n^3)^4 \sum_{k=1}^{\infty} x_k^2 \sin^2 \left(\frac{\pi k}{\omega n^3} \right) \left| \sum_{s=1}^{\infty} i^s J_s \left(\frac{3\epsilon n k}{\omega} \right) \times \frac{s^2}{k^2 - (s\omega n^3)^2} \right|^2 \quad (2.6)$$

Equating (2.6) with the square of the condition (2.4) we obtain an implicit equation for the critical ionization field:

$$1 = 128 f^2 (\omega n^3)^2 \sum_{k=1}^{\infty} x_k^2 \sin^2 \left(\frac{\pi k}{\omega n^3} \right) \left| \sum_{s=1}^{\infty} i^s J_s \left(\frac{3\epsilon n k}{\omega} \right) \times \frac{s^2}{k^2 - (s\omega n^3)^2} \right|^2 \quad (2.7)$$

Since (2.6) tells only about the mean square spread in n and nothing about fluctuations around this mean spread, we introduced a factor f , which has to be adjusted to the data, and takes care of the fact that the excursion of some trajectories, at a given field, might be considerably larger than the mean excursion given by (2.6). We used (2.7) to calculate the critical fields as a function of the initial n value, and obtained the results shown in Fig. 2 where the value $f = 2.5$ was found to give the best overall agreement with the data. The value of f can also be estimated by considering the critical ionization field in the static limit, i.e., $\omega \rightarrow 0$. In this limit the sums in (2.7) can be calculated analytically and upon replacing the strongly oscillating \sin^2 -term by its mean value $1/2$ one gets the result:

$$\epsilon n^4 = 0.26/f \quad (2.8)$$

Since in the static limit ϵn^4 approaches 0.13, we have to choose $f \approx 2$ which is not far from the value obtained phenomenologically.

The perturbative approach which led to (2.7) measures the mean excursion of an ensemble of trajectories rather than the width of resonances and is therefore different from Chirikov's method, which was successfully used to predict the onset of ionization in the $\omega n^3 > 1$ domain [14, 19] and which we extended with some success to the $\omega n^3 < 1$ -region. The two methods are in a sense complementary.

The result (2.7) can be also viewed quantum mechanically. By using the interaction representation to be defined in the next chapter together with first order perturbation theory, we calculate the probability that a transition from the initial state n to any other state m occurs within one field cycle. We get:

$$P_{n \rightarrow m} = \frac{16\epsilon^2 z_{nm}^2}{\omega^2 y_{nm}^2} \sin^2(\pi \Delta_{nm}) \left| \sum_{s=1}^{\infty} \frac{s^2}{s^2 - \Delta_{nm}^2} i^s J_s(y_{nm}) \right|^2 \quad (2.9)$$

where

$$y_{nm} = \frac{3\epsilon}{2\omega} (m^2 - n^2), \quad \Delta_{nm} = \frac{1}{2\omega} \left(\frac{1}{n^2} - \frac{1}{m^2} \right) \quad (2.10)$$

and z_{nm} stand for the matrix elements of the dipole operator. We use the transition probabilities (2.9) to calculate quantum mechanically the spread in n :

$$(\Delta n)^2 = \sum_{k=1-n}^{\infty} k^2 P_{n \rightarrow n+k} \quad (2.11)$$

For large n and $k \neq 0$ we have:

$$\frac{z_{n,n+k}}{n^2} = -J'_k(k)/k = -x_k, \quad \Delta_{n,n+k} = \frac{k}{\omega n^3},$$

$$y_{n,n+k} = \frac{3\epsilon n k}{\omega} \quad (2.12)$$

Inserting (2.12) into (2.9) we obtain from (2.11) exactly the classical result (2.6) for the mean square spread in n .

In Fig. 2 we used the expression (2.11) rather than its purely classical analogue. The two expressions differ only at low values of n where the semi classical correspondence (2.12) is least justified.

In summary, we have shown that the classical dynamics in the bound space shows three distinct patterns depending on the action variable n . At low n , the atom is not affected by the presence of the driving field and the motion is regular. At high n values the motion is regular due to the dominance of the field term over the unperturbed Hamiltonian. There exists a rather narrow domain in phase-space where both terms in the Hamiltonian are of comparable strength, and this is where classical chaos shows. The lower n border of this region determines the onset of ionization, and an analytical expression was derived based on an appropriate perturbation expansion which differs from the standard resonance overlap criterion. In the next chapter we shall show how these features find their expression in the quantum picture of the ionization process.

3. Quantum mechanical theory

The periodic dependence of the driving field on time enables us to write the wave function after the application of N microwave cycles in the form of a quantum mapping [28]:

$$|\psi(N)\rangle = U^N(T) |\psi(0)\rangle \quad (3.1)$$

where $U(T)$, $T = 2\pi/\omega$, denotes the 1-cycle time evolution operator and $|\psi(0)\rangle$ is the initial state of the atom. Of central importance for the quantum description of the probability flow is the nature of the eigenvectors $|\alpha\rangle$ of the 1-cycle propagator U . Since U is unitary, the eigenvalue problem can be written in the form:

$$U|\alpha\rangle = e^{-i\omega_\alpha} |\alpha\rangle \quad (3.2)$$

where the real quantities ω_α are called the quasi energies and $|\alpha\rangle$ are the quasi energy or Floquet states [29]. If we use the spectral decomposition of U , the amplitude $b_n(N)$ to excite any given state $|n\rangle$ after N cycles of the microwave field and for initial condition $|\psi(0)\rangle = |n_0\rangle$ is given by:

$$b_n(N) = \langle n | U^N(T) | n_0 \rangle = \sum_{\alpha} \langle n | \alpha \rangle e^{-iN\omega_\alpha} \langle \alpha | n_0 \rangle \quad (3.3)$$

Hence, in order to enable a $n_0 \rightarrow n$ transition, there has to be at least one Floquet state $|\alpha\rangle$ which connects *both*, $|n\rangle$ and $|n_0\rangle$. In other words, the degree of localization or delocalization of the quasi energy states $|\alpha\rangle$ will determine the efficiency by which the atom absorbs energy from the external microwave field. In the localized situation, the induced excitation is limited, whereas if delocalized quasi energy states overlap with the initial state $|n_0\rangle$ of the atom, energy can be absorbed efficiently until the atom finally ionizes.

The understanding of the structure of the Floquet states is

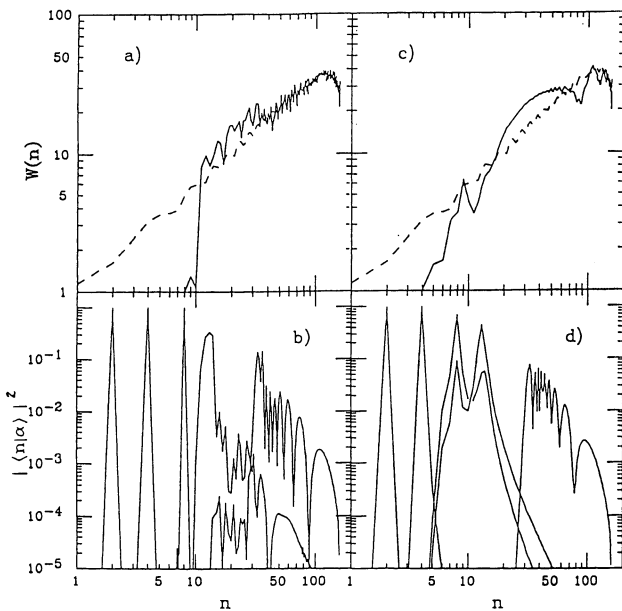


Fig. 5. (a) Width-function and (b) some typical quasi energy states, calculated in a basis of 160 bound states, for $\varepsilon = 10^{-5}$ and $\omega = 5 \times 10^{-5}$. (c) and (d): same as (a) and (b) respectively, but for $\varepsilon = 5 \times 10^{-5}$ and $\omega = 5 \times 10^{-3}$. Basis truncation effects become serious for $n \gtrsim 100$.

the main objective in the study of the quantum dynamics of classically chaotic systems. In the case of the kicked rotor, the localization of these states is responsible for the quantum suppression of the diffusion of energy. The mechanism which brings about the exponential localization was identified as being analogous to the Anderson mechanism [2]. The relation between the diffusion constant and the localization length was amply discussed by the previous lecturer. We shall present now our results concerning the driven hydrogen atom, and show that in the present system there are other physical effects which produce different localization properties.

The discussion of the Floquet spectrum in the present problem is encumbered by the existence of the continuum in the spectrum of the unperturbed atom. To make a meaningful comparison with the kicked rotor and with the classical theory of the preceding chapter, we limit the discussion here to the dynamics in the space spanned by the bound states of the atom. This is the analogue of the region of phase-space described in terms of action-angle variables. When we discuss the ionization process, we shall reinstate the continuum in its due place.

Figure 5(b) and Fig. 5(d) show the overlaps of some typical eigenstates $|\alpha\rangle$ of the 1-cycle propagator in the $|n\rangle$ basis for two different sets of field parameters. We see that the quasi energy states can be grouped into 3 categories, which have been dubbed Type I, II and III in Ref. [4]:

(I) States which overlap mainly with low n states and which differ very little from the original free atom states (narrow states),

(II) transitional states, and

(III) states which overlap mainly with high n states and whose expansion amplitudes decay as a power of n for large n (broad states).

The spectrum of the 1-cycle propagator will always contain Type I and Type III states whereas the range of transitional states depends on the field parameters (compare

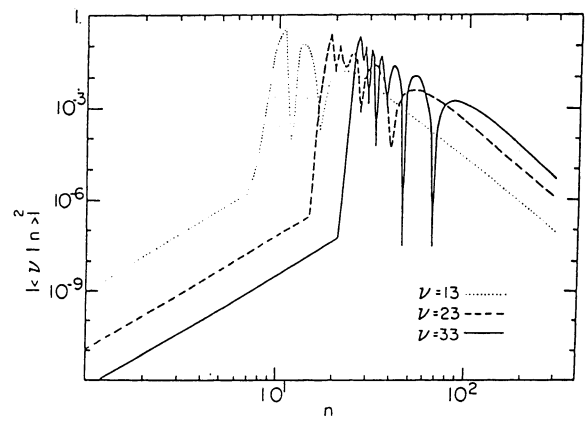


Fig. 6. Some typical eigenstates of the bound space projected dipole operator \hat{z} .

Fig. 5(b) and Fig. 5(d)) and can be very narrow (see Fig. 5(b)).

The transition stems from the same dynamical reasons which affect a similar transition in the classical treatment. Type I Floquet states are the quantum analogues of the regular periodic orbits at low n values. The Type III Floquet states correspond to the U-shaped classical trajectories at high n values while Type II states play the role of the chaotic strip observed in the intermediate range of n values in the classical phase portrait (see Fig. 3). Because of the dominance of the z operator in the high n domain, we studied the spectral properties of the operator z in the entire space of bound eigenstates $|n\rangle$ [16]. By a semi-classical quantization of the $z(n, \Theta) = \text{const.}$ trajectories and detailed numerical investigations we could show that the spectrum of the z operator is discrete and we derived the following properties for its eigenvalues ζ_ν and eigenvectors $|v\rangle$:

- (1) $\zeta_\nu = \pi^2/8 (\nu + 1/4)^2$, $\nu = 1, 2, \dots$

- (2) $\langle n|v\rangle$ is exponentially small for $n < \pi/4 (\nu + 1/4)$. At $n = \pi/4 (\nu + 1/4)$ it rises abruptly to its maximal value.

- (3) Beyond this limiting value of n , the expansion coefficients $\langle n|v\rangle$ change sign a few times and finally decay as $n^{-5/2}$ for large n . The last zero of the oscillations occurs at $n = \pi/(4\sqrt{6}) (\nu + 1/4)^{3/2}$.

Typical eigenstates of the z operator are shown in Fig. 6. Comparing the quasi energy states in the “Type III” – region in Fig. 5 with the z -eigenstates of Fig. 6, we see that the picture of a transition from H_0 – dominated motion to z -motion holds very well indeed.

We shall now use perturbation theory to get an estimate for the critical value n_c at which the transition between Type I and Type II states is expected to occur. The eigenvalue problem (3.2) can be posed in an alternative way. We obtain the quasi energy states $|\alpha\rangle$ by solving the Schrödinger equation subject to the boundary condition:

$$|\alpha(T)\rangle = e^{-i\omega\alpha} |\alpha(0)\rangle; |\alpha(0)\rangle \equiv |\alpha\rangle \quad (3.4)$$

It is useful to split the interaction term in the Hamiltonian (2.1) into a “diagonal” and an “off-diagonal” part:

$$V(z, t) = V_D(z, t) + V_N(z, t) = \varepsilon \cdot z \cdot \sin(\omega t)$$

$$\langle n|V_D(t)|m\rangle = \begin{cases} \frac{3}{2}\varepsilon n^2 \sin(\omega t), & n = m \\ 0, & n \neq m \end{cases} \quad (3.5)$$

$$\langle n | V_N(t) | m \rangle = \begin{cases} 0, & n = m \\ \varepsilon \langle n | z | m \rangle \sin(\omega t), & n \neq m \end{cases}$$

The perturbation expansion is carried out in the interaction representation:

$$|\alpha(t)\rangle = \exp \left[-i \left(H_0 t + \int_0^t V_D(t') dt' \right) \right] |\alpha_i(t)\rangle \quad (3.6)$$

where the effect of the large diagonal part of the interaction $-V_D(t)$ is extracted explicitly. This procedure is the quantum analogue of the classical theory which led to (2.6). The form (3.6) is substituted into the time dependent Schrödinger equation. Integrating both sides of the equation along one cycle of the field and imposing the condition (3.2) we obtain:

$$\left\{ \exp \left[i \left(H_0 T + \int_0^T V_D(t') dt' \right) - i\omega_x \right] - 1 \right\} |\alpha_i(0)\rangle \\ = \frac{1}{i} \int_0^T \tilde{V}_I(t') |\alpha_i(t')\rangle dt' \quad (3.7)$$

where $\tilde{V}_I(t)$ is the interaction representation of the non-diagonal part of $V(z, t)$.

In the low n regime, we start the perturbation expansion by setting $|\alpha_i(t)\rangle = |n\rangle$. Then, $\omega_x = -1/(2n^2)T$ and the quasi energy state $|\alpha^{(n)}\rangle$ which is centered on $|n\rangle$ is distributed on $m \neq n$ states according to:

$$|\langle m | \alpha^{(n)} \rangle| = \left| \frac{2\varepsilon z_{nm}}{\omega y_{nm}} \sum_{s=1}^{\infty} (-i)^s \frac{s^2}{s^2 - \Delta_{nm}^2} J_s(y_{nm}) \right| \quad (3.8)$$

where z_{nm} are the matrix elements of the dipole operator and y_{nm} and Δ_{nm} were defined in equation (2.10). The Floquet state $|\alpha^{(n)}\rangle$ is localized on $|n\rangle$ as long as the amplitudes (3.8) are small. Except for resonance conditions, the largest amplitudes occur for $m = n \pm 1$. The critical n at which localization breaks down, is estimated as the value $n = n_t$ for which [30]

$$|\langle n_t + 1 | \alpha^{(n_t)} \rangle| = 1/2 \quad (3.9)$$

Using the leading terms in (3.8) and $z_{n,n+1} \approx -\frac{1}{3}n^2$, we get

$$\frac{1}{2} = \left| \frac{\frac{1}{3}\varepsilon\omega n_t^8}{1 - (\omega n_t^3)^2} \cdot \left(1 - i \cdot \frac{1 - (\omega n_t^3)^2}{1 - (2\omega n_t^3)^2} \cdot \frac{3\varepsilon n_t}{\omega} \right) \right| \quad (3.10)$$

Extensive numerical calculations show that in the parameter range of interest here, the formula (3.10) reproduces the transition points to better than ± 5 states. We used (3.10) to calculate n_t for the parameters used in Fig. 1 of Ref. [31]. The resulting $n_t = 73$ agrees remarkably well with the n value where the probability distribution in this figure exhibits the sharp transition.

A non-perturbative estimate of the transition point n_t is obtained by calculating numerically the 1-cycle propagator and diagonalizing it in a sufficiently large space of basis functions. In order to extract the transition point from the numerical data, it is useful to introduce an objective measure for the extension of an unperturbed state $|n\rangle$ when expanded in the quasi energy basis $\{|\alpha\rangle\}$. We define the width function [32]:

$$W(n) = \exp \left[- \sum_{\alpha} |\langle \alpha | n \rangle|^2 \ln |\langle \alpha | n \rangle|^2 \right] \quad (3.11)$$

It is assumed that $\sum_{\alpha} |\langle \alpha | n \rangle|^2 = 1$. $W(n)$ gives the effective

number of states used in the expansion of the state $|n\rangle$ in the basis $\{|\alpha\rangle\}$. Fig. 5(a) and Fig. 5(c) show the width $W(n)$ for two different sets of fields and frequencies. In both cases we observe that for small enough n , $W(n)$ is approximately 1 and grows linearly in n for large n . This behavior can be explained on the basis of our picture of a cross-over from H_0 -dominated motion to z -dominated motion as a function of increasing n . For low n , the external microwave field is very weak compared to the atomic binding field, and the spectra of H_0 and of U are nearly the same. In this case, a single quasi energy corresponds almost uniquely to a single unperturbed state $|n\rangle$ resulting in $W(n) = 1$. For large n , z -motion will take over and the spectrum of the 1-cycle operator U will resemble the eigenstates of the dipole operator. One can show analytically in this case, using the definition of the width function (3.11) and the spectral properties of the z -eigenstates that the width of an unperturbed state $|n\rangle$ expanded in the set of eigenstates $|\nu\rangle$ of the z -operator grows linearly with n . The dashed lines in Fig. 5(a) and Fig. 5(c) are the width of a state $|n\rangle$ in the eigenbasis of z and the fact that the width of $|n\rangle$ in the quasi energy basis (full lines) approaches the dashed lines asymptotically, provides further evidence that the quasi energy states which overlap appreciably with the high n states approach the z -eigenstates $|\nu\rangle$ for large n .

The parameters in Fig. 5 were chosen in such a way that in both cases the transition points were expected to occur around $n \approx 10$, but $\omega n_t^3 < 1$ for Fig. 5(a, b) and $\omega n_t^3 > 1$ for Fig. 5(c, d). It can be seen that the two conditions lead to quite a different qualitative behavior of the transition region between the two regimes $W(n) \cong 1$ and $W(n) \sim n$. In the case $\omega n_t^3 < 1$ we observe a very characteristic, steep rise of the width function $W(n)$ at $n = n_t$, whereas in the case $\omega n_t^3 > 1$ the transition is much more gentle. At this point we note that for all the hydrogen ionization experiments conducted so far [5–11], $\omega n_t^3 \gtrsim 1$ is always fulfilled and according to Fig. 5(a), the critical value n_t , which marks the transition point between the H_0 - and z -dominated regimes, is very well defined. One can establish a correspondence between any given n value and the critical field ε_c for which the transition occurs at the chosen n . This can be done numerically by extracting the information from the width function, or perturbatively using (3.10). The result of such a procedure is shown in Fig. 7 where the stars are extracted from the numerical calculations while the full line shows the critical field evaluated from (3.10). The perturbative estimate of the critical field is less accurate in the vicinity of the 1, 2, . . . -photon resonances at $n = 87, 69, \dots$ respectively. This is expected on the basis of the crude criterion chosen to determine n_t . The overall agreement is rather convincing and shows that the transition from localized states to “broad” states in this regime of parameters is perturbative.

We may repeat now the perturbative calculation of the Floquet eigenstates choosing the representation where the operator z is diagonal. Assuming a z eigenvector to represent the Floquet state to zeroth order, one finds that the mixing of neighboring z eigenstates due to the presence of H_0 is $\sim 1/\sqrt{N}$ for large enough N values. This substantiates the claim that the Floquet states which overlap appreciably with high n states approach in the limit the z eigenstates $|\nu\rangle$.

Because of their asymptotic approach to the z -eigenstates, the components of the quasi energy states in the bound space are always normalizable. Technically speaking, the quasi

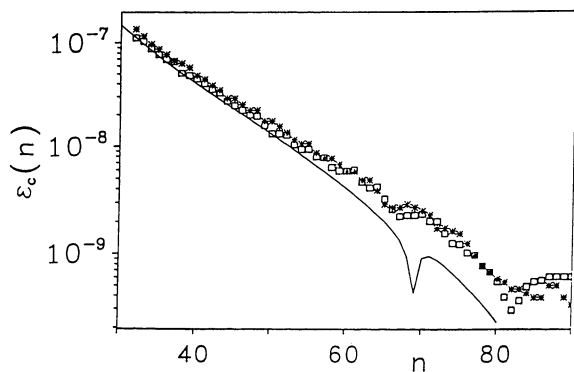


Fig. 7. The critical field $\varepsilon_c(n)$ as a function of the initial state n . Squares: Experimental results for the critical 10% ionization fields [8–11]. Stars: numerical evaluation of the field at which the transition from narrow to broad states occurs at the given n . Full line: Second order perturbation theory (Eq. (3.10)). The experiment and the calculations were carried out at $\omega = 1.509 \times 10^{-6}$.

energy states are never “delocalized” but, because of the powerlaw fall off, they are only marginally localized. This contrasts with the suggestion [4] that among the quasi energy states there should exist localized as well as delocalized states. This claim was based on a seemingly erratic behavior of the quasi energy states in the “Type III”-region. In view of Fig. 5 we have to conclude that the basis in Ref. [4] was far insufficient to see the powerlaw decay of the states in the “Type III”-region. Such a transition from “narrow” to “broad” states seems to be quite a common phenomenon, and it occurs e.g., in the system of periodically kicked surface state electrons [32].

The existence of a value n_t at which there is a transition from narrow (H_0 dominated) to broad (z dominated) states, is closely linked with the onset of ionization. We have shown [16] that as long as its rate is low, the ionization process can be viewed as a two-step process. First, probability has to be transferred to “door-way” states which then ionize. We found that for a given field strength the door-way states lie above $n_\omega = (1/3\varepsilon)^{1/4}$. Ionization may occur only if probability is transferred to states with $n > n_\omega$. For low fields ε the initial state $|n_0\rangle$ is nearly an eigenstate of the 1-cycle operator U . Therefore it cannot feed higher lying states and since $n_0 < n_\omega$ it cannot decay directly to the continuum. Consequently the atom is stable under the external perturbation with no resulting ionization. Increasing the field strength ε , but keeping $n_0 < n_\omega$, the direct route to the continuum is still barred, but an alternative route opens at some critical field ε_c where the width of the state $|n_0\rangle$ increases to the maximal value which the operator z can induce. Suddenly many quasi energy states are needed for an expansion of the initial state $|n_0\rangle$, and these states, being close to the eigenstates of the z -operator, decay only as a power law and provide an efficient link between the initial state $|n_0\rangle$ and the states with $n > n_\omega$. Via this link, the probability which was initially concentrated in the state $|n_0\rangle$ is efficiently transported upwards to the door-way states from where it decays with appreciable rates to the continuum. Thus the critical field for ionization should coincide with the transition field ε_c defined above. The squares in Fig. 7 are the measured critical fields for ionization. The agreement between the theoretical estimate and the measured values is very good.

The mechanism outlined above, provides an overall expla-

nation for the onset of strong ionization as a function of the microwave field strength. In a number of cases, however, the experimental ionization curves show structures for field strengths well below the critical ionization field ε_c (see e.g., Fig. 1(b–d)). The mechanism responsible for this effect is different from the one discussed above and will be shown to be of purely quantum origin.

Below the critical ionization field ε_c there are no Floquet states which overlap with both the initial state and with $n > n_\omega$ states. Consider two Floquet states $|\alpha\rangle$ and $|\beta\rangle$ such that

$$\begin{aligned} |\langle n_0|\alpha\rangle| &= A \sim 1; & |\langle n_\omega|\beta\rangle| &= B \sim 1; \\ |\langle n_0|\beta\rangle| &\sim 0; & |\langle n_\omega|\alpha\rangle| &\sim 0 \end{aligned} \quad (3.12)$$

The corresponding Floquet eigenvalues are functions of the field strength. If at some value ε the eigenvalues display an avoided crossing, the Floquet eigenstates mix very effectively and the transition $n_0 \rightarrow n_\omega$ can occur. Avoided crossings happen at well defined field values and their effect is confined to a narrow range of field strengths in the vicinity of the crossing. In actual experiments the effect of a single avoided crossing cannot be noticed unless an extremely accurate experimental set-up is designed. It so happens that under special conditions some 10–30 avoided crossings occur in a narrow range of the field strength, which is presently of the order of the experimental field resolution. This clustering of avoided crossings produces enhanced ionization which is observed experimentally as sub-threshold ionization peaks. In Fig. 1 we show the experimental ionization curve for $n = 38$ together with two theoretical curves. The smoothed curve was obtained from the spiky one by convolution with the experimental uncertainty in the determination of the field. A detailed check of the Floquet spectrum showed that to each spike in the theoretical ionization curve there corresponds an avoided crossing of Floquet eigenstates which have the property (3.12) before and after the avoided crossing.

Subthreshold structures were observed for various other n values and the quantum theory always reproduced their location and relative heights. These results substantiate the qualitative validity of our interpretation of the subthreshold ionization resonances as being due to an enhanced excitation of the $n > n_\omega$ states at selected field values where avoided crossings of quasi energies occur.

Till this point we limited the discussion to the dynamics in the bound space. We have developed a calculational scheme which includes the ionization channel, and the theoretical ionization curves presented in Fig. 1 are the result of such calculations. We found that the inclusion of the continuum does not change substantially the bound space dynamics, even though now the probability to remain bounded decreases with time.

4. Summary and conclusions

The main conclusion of this work is that but for the sub-threshold ionization phenomenon, the classical and the quantum theories of the microwave ionization of the hydrogen atom reproduce equally well the ionization data in the domain $\omega n^3 < 1$. The two theories show the same transition from H_0 dominated motion to $z = \text{const.}$ motion, and the onset of ionization just signals that the initial n value makes the transition from one phase to the other when the field

equals $\varepsilon_c(n)$. Perturbative estimates which convey the same physical idea but expressed using either the classical or the quantal language were derived and found to be consistent with the data. In this domain of field parameters, we could not find any evidence for the "quantal suppression of classical diffusion" which is present in other systems. This is probably due to the fact that the transition between the two asymptotic regimes is rather abrupt for the cases studied here. A different behavior was observed in the studies of the complementary range of parameters ($\omega n^3 > 1$) where the transition between the asymptotic regimes is gradual and Type II states play a more important role.

As for the localization properties of the Floquet states in the $\omega n^3 < 1$ -domain, the Anderson mechanism has little effect if any. The Floquet states are normalizable and the Type I and Type III states are perturbatively localized on eigenstates of H_0 and z respectively. Only the Type II states, of which there is only a finite number, may show a local exponential decay. There, one might try to connect the classical diffusion coefficient in the chaotic strip and the localization length of Type II states. This deserves further study.

The only genuine quantum effect observed so far are the sub-barrier ionization peaks. The avoided crossing mechanism which is responsible for these effects was also identified in the study of the microwave excitation of diatomic molecules [33]. The occurrence of avoided crossings is a manifestation of the fluctuations in the Floquet spectrum. The study of the statistical properties of the Floquet spectra is still in its infancy, and it may lead to interesting links in the study of quantum chaos of static and periodically driven systems.

Acknowledgements

We would like to thank Profs. P. M. Koch and R. V. Jensen for kindly providing their latest experimental and numerical data. We profited from discussions and correspondence with Profs. W. C. Shieve and I. Guarneri. This research was supported in part by the Israeli Basic Research Commission.

References

1. Casati, G., Chirikov, B. V., Izrailev, F. M. and Ford, J., in Lecture Notes in Physics, Springer, New York, Vol. 93, p. 334 (1979).
2. Fishman, S., Grempel, D. R. and Prange, R. E., Phys. Rev. Lett. **49**, 509 (1982); Grempel, D. R., Prange, R. E. and Fishman, S., Phys. Rev. **A29**, 1639 (1984).
3. Chirikov, B. V., Phys. Rep. **52**, 263 (1979).
4. Bardsley, J. N., Sundaram, B., Pinnaduwaige, L. A. and Bayfield, J. E., Phys. Rev. Lett. **56**, 1007 (1986).
5. Bayfield, J. E. and Pinnaduwaige, L. A., Phys. Rev. Lett. **54**, 313 (1985) and J. Phys. **B18**, L49 (1985).
6. Bayfield, J. E. and Koch, P. M., Phys. Rev. Lett. **33**, 258 (1974); Bayfield, J. E., Gardner, L. D. and Koch, P. M., Phys. Rev. Lett. **39**, 76 (1977).
7. Koch, P. M., J. Physique (Paris) **43**, Colloq. C2-187 (1982).
8. Koch, P. M., in "Fundamental Aspects of Quantum Theory" (Edited by V. Gorini and A. Frigerio), Plenum Press, NY (1986).
9. van Leeuwen, K. A. H., Oppen, G. v., Renwick, S., Bowlin, J. B., Koch, P. M., Jensen, R. V., Rath, O., Richards, D. and Leopold, J. G., Phys. Rev. Lett. **55**, 2231 (1985).
10. Koch, P. M., van Leeuwen, K. A. H., Rath, O., Richards, D. and Jensen, R. V., Proceedings of the First International Conference on the Physics of the Phase Space, Univ. of Maryland, 20-23 May, 1986, to be published in "Physics of the Phase Space", Lecture Notes in Physics (Springer, 1987).
11. Koch, P. M., private communication.
12. Delone, N. B., Zon, B. A. and Krainov, V. P., Zh. Eksp. Teor. Fiz. **75**, 445 (1978); Sov. Phys. JETP **48**, 223 (1978).
13. Meerson, B. I., Oks, E. A. and Sasarov, P. V., Pis'ma Zh. Eksp. Teor. Fiz. **29**, 79 (1979); JETP Lett. **29**, 72 (1979).
14. Delone, N. B., Krainov, B. P. and Shepelyansky, D. L., Usp. Fiz. Nauk. **140**, 355 (1983); Sov. Phys. Usp. **26**, 551 (1983), and references therein.
15. Blümel, R. and Smilansky, U., Physica Scripta **35**, 15 (1987).
16. Blümel, R. and Smilansky, U., Zeit. f. Phys. **D6**, 83 (1987).
17. Blümel, R., Smilansky, U., van Leeuwen, K. A. H., Koch, P. M., Richards, D. and Leopold, J. G., submitted to Phys. Rev. Lett. (1987).
18. Pillet, P., van Linden van den Heuvell, H. B., Smith, W. W., Kachra, R., Tran, N. H. and Gallagher, T. F., Phys. Rev. **A30**, 280 (1984).
19. Jensen, R. V., Phys. Rev. Lett. **49**, 1365 (1982); Phys. Rev. **A30**, 386 (1984).
20. Shepelyansky, D. L., in Chaotic Behavior in Quantum Systems (Edited by G. Casati), p. 187, Plenum, New York (1985).
21. Casati, G., Chirikov, B. V., Shepelyansky, D. L. and Guarneri, I., Phys. Rev. Lett. **57**, 823 (1986).
22. Leopold, J. G. and Percival, I. C., J. Phys. **B12**, 709 (1979).
23. Leopold, J. G. and Richards, D., J. Phys. **B18**, 3369 (1985).
24. Rath, O. and Richards, D., in preparation.
25. Jensen, R. V., Oji Int. Sem. on Highly Excited States of Atoms and Molecules, Fuji-Yoshida, Japan (1986).
26. Jensen, R. V., Proceedings of the Adriatico Research Conference on Quantum Chaos, Physica Scripta (1987); Sanders, M. M. and Jensen, R. V., in preparation.
27. Blümel, R. and Smilansky, U., in preparation.
28. Berry, M. V., Balazs, N. L., Tabor, M. and Voros, A., Ann. Phys. **122**, 26 (1979); Zaslavsky, G. M., Phys. Rep. **80**, 158 (1981).
29. Zeldovich, Ya. B., Sov. Phys. JETP **24**, 1006 (1967); Chu, S., J. Chem. Phys. **75**, 2215 (1981); Dion, D. R. and Hirschfelder, J. O., Adv. Chem. Phys. **35**, 265 (1976); Gesztesy, F. and Mitter, H., J. Phys. **A14**, L79 (1981).
30. Hose, G. and Taylor, H. S., Phys. Lett. **51**, 947 (1983).
31. Casati, G., Chirikov, B. V., Guarneri, I. and Shepelyansky, D. L., Phys. Rev. Lett. **56**, 2437 (1986).
32. Blümel, R. and Smilansky, U., Phys. Rev. Lett. **52**, 137 (1984); Phys. Rev. **A30**, 1040 (1984).
33. Blümel, R., Fishman, S. and Smilansky, U., J. Chem. Phys. **84**, 2604 (1986).